LIMNOLOGY
and
OCEANOGRAPHY: METHODS

Limnol. Oceanogr.: Methods 3, 2005, 247–262

A multi-platform bathyphotometer for fine-scale, coastal bioluminescence research

Christen M. Herren[1], Steven H.D. Haddock[1], Cyril Johnson[2], Cristina M. Orrico[3], Mark A. Moline[4], and James F. Case[3]*

[1]Monterey Bay Aquarium Research Institute, 7700 Sandholdt Rd., Moss Landing, CA 95039, USA
[2]Department of Physics, University of California Santa Barbara, Santa Barbara, CA 93106, USA
[3]Marine Science Institute, University of California Santa Barbara, Santa Barbara, CA 93106, USA
[4]Biological Sciences Department, California Polytechnic State University, San Luis Obispo, CA 93407, USA

Abstract

Although bioluminescence (BL) in the open ocean has been extensively studied, coastal BL remains poorly understood due, in large degree, to a lack of BL instrumentation appropriate to measure the fine-scale biological and physical complexity of the coastal regime. As a contribution toward understanding coastal BL, we developed the Multipurpose Bioluminescence Bathyphotometer (MBBP). This compact, self-contained bathyphotometer (BP) was designed to function in a variety of deployment modes, including conventional shipboard profilers, towed platforms, autonomous underwater vehicles (AUVs), and profiling moorings. In all configurations, the instrument preserves signal structure at centimeter to meter scale resolution, the scale at which higher-flow instruments might disturb thin layers and other fine-scale water column features. In the MBBP, seawater is conveyed with minimal premeasurement excitation into a light-baffled stimulation and measurement chamber at a continuously measured flow rate of 350 to 400 mL s^{-1}. A photomultiplier tube (PMT) records light from bioluminescent organisms after they are mechanically stimulated at the chamber entrance by a high-velocity impeller. Calibration and test protocols were developed to determine BL stimulation efficiency and MBBP measurement characteristics. To illustrate the capabilities of the MBBP to resolve the fine-scale structure of the BL community, measurements from two coastal environments are presented.

Marine bioluminescent organisms occur at all accessible depths and domains, often in immense numbers (Herring 2002). Although the sources and occurrence of oceanic bioluminescence (BL) have been extensively studied, poorly characterized instruments have often been involved, raising questions regarding radiometric and excitational inter-calibration. While there is currently only one commercially available bathyphotometer, the Glowtracka™ (Chelsea Instruments, evolved from Aiken and Kelly 1984), there exists a wide variety of custom-built bathyphotometers (BPs) that were designed for specific purposes and have been fabricated in small numbers (Table 1) (*See* also Batchelder and Swift 1989; Batchelder et al. 1990; Batchelder et al. 1992; Case et al. 1993; Gitel'zon et al. 2000; Greene et al. 1992; Lapota et al. 1988, 1989, 1992; Lapota 1998; Lieberman et al. 1987; Losee et al. 1989; Rudyakov 1968, Swift et al. 1983, 1988, 1995; Widder et al. 1992). Because these instruments employ varied excitation, measurement, and calibration protocols, standardization among them is not readily attainable and some of them no longer exist. It should be noted that we do not consider here open-volume BPs (Boden et al. 1965) because accurate radiometric measurements are essentially impossible, even when the instrument is designed for coincident counting of a distant volume.

Increased scientific and applied interest in coastal processes currently stimulates much research on BL in near-shore plankton communities (Blackwell et al. 2002; Shulman et al. 2003). The numerical and biogeographic importance of BL in ocean

*Corresponding author. E-mail: case@lifesci.ucsb.edu

Acknowledgments

J. Bellingham, H. Thomas, M. Sibenac, A. Briggs, E. Heine, S. Blackwell, A. Alldredge, D. V. Holliday, P. Donaghay, J. Sullivan, and O. Schofield made valued contributions to data collection efforts. We are grateful to J. Brewster, A. Briggs, A. Bass, K. Maynard, and S. MacIntyre for timely assistance in data analysis and manuscript preparation. Suggestions by M. Latz, C. McDougall, P. Girguis, S. Blackwell, and three anonymous reviewers improved this manuscript considerably. The engineering design, development, and field trials involved in this work were supported by the UCSB Electronics and Machine Shop staff, and the crews of the RV *Pt Sur*, RV *Walford*, and RV *Acoustic Explorer*. Support of the Office of Naval Research is gratefully acknowledged: AASERT N00014-97-1-0798 to C.H. and J.F.C., N00014-97-1-0424 to J.F.C., N00014-00-1-0842 to S.H., and N00014-00-1-0008 to M.M. and N00014-00-10570 M.M. We are indebted to the University of California Santa Barbara, California Polytechnic State University at San Luis Obispo, the Monterey Bay Aquarium Research Institute, and Rutgers University LEO-15 research groups for access to invaluable research resources. J.F.C. is indebted to the FBN Fund.

Table 1. Salient stages in the development of closed volume bioluminescence bathyphotometers

Source	Name	Deployment mode	Excitation	Flow	Inlet diameter (cm)	Residence time (ms)	Measuring volume (L)
Clark and Kelly (1965)	NA	Profiler (to 2000 m)	Impeller	0.37 L s^{-1}	2.5	500	NA
Soli (1966)	NA	Shallow near-shore profiling	Impeller facing detector	Variable	2.54	NA	0.1*
Seliger et al. (1969)	NA	Towed from small boat	Impeller	0.2 L s^{-1}	1.3	225	NA
Hall and Staples (1978)	NA	Profiler (to 200 m)	Constriction turbulence, pump	NA	NA	25*	0.025*
Aiken and Kelley (1984)	GlowTracka (Chelsea Inst. Ltd., commercial version)	Ship towed, undulating profiler (to 1000 m)	Inlet flowmeter turbulence	1-5 dm^3 s^{-1} at 5 m s^{-1} tow speed	2.8	25	0.02
Greenblatt et al. (1984); Losee et al. (1985)	NA	Profiling, various shipboard modes	Constriction turbulence	1.1 L s^{-1}	1.6	20	0.025
Nealson (1985)	JHU/APL-BP	Profiler (to 300 m), towed paravane, shipboard surface mapping	Inlet 90° baffles	1 L s^{-1}	2.5	200	0.10
Swift et al. (1985)	NA	Profiler	Impeller	0.25 L s^{-1}	1.4	1000	NA
Buskey (1992)	Univ. of Texas HIDEX-type BP	Profiler	Inlet grid	6.3 L s^{1}	NA	750	4.7
Widder et al. (1993)	HIDEX	Profiler	Inlet grid	16-44 L s^{-1} (max)	12	260-5,200	11.3
Neilson et al. (1995)	MOORDEX	Sea mooring	Inlet propeller or natural surge	1-12 L s^{-1}	12.7	Surge dependent	5
Fucile (1996)	SSBP	Free-fall retrievable profiler (2 ms^{-1})	Inlet grid, Nitex 1800 μm	15.7 L s^{-1}*	10	140	2
Geistdoerfer and Vincendeau (1999)	NA	Profiler (to 600 m)	Inlet grid	0.5 L s^{-1}	1.7	450	0.19
McDuffey and Bird (2002); Losee et al. (1985)	Biolite	Underway shipboard	Constriction turbulence	1 L s^{-1}	1.3	49	0.049
Bivens et al. (2002); Gieger (personal communication)	OTiS	Profiler	Constriction turbulence	1 L s^{-1}	1.5	25	0.025
Herren (this publication)	MBBP-G2	Multiplatform	Impeller	0.5 L s^{-1}	3.2	10,000	0.5

[a]Estimated value.

biodynamics is strongly reinforced by remarkable biochemical evidence that BL evolved independently, principally in the sea, as many as 30 times (Hastings 1983). Moreover, there is evidence for the adaptive significance of this phenomenon (Case et al. 1995). In spite of this, except for the vigorous attention paid to luminescence by Soviet-era oceanographers (i.e., from Tarasov and Gitel'zon 1961 to Utyushev et al. 1999), most biological oceanographic research by Western oceanographers lacked these measurements, unless BL was a specific research target, as in the prescient US Office of Naval Research Biowatt I and II research initiatives (Marra and Hartwig 1984). Luminescence measurements have the potential to estimate a

portion of plankton biomass *in situ* and thereby contribute to an understanding of plankton population dynamics (Lapota 1998; Piontkovski et al. 1997). There is now a growing body of research on BL population dynamics and prediction achieved with major deployments of BL detectors (Haddock et al. 2004, 2002, 2001; Shulman et al. 2003).

Bathyphotometers have provided information about bioluminescent organisms, specifically the spatial and temporal location of BL as well as its relationship with other measured biological, physical, and chemical parameters in the ocean (e.g., Neilson et al. 1995; Widder et al. 1999; McManus et al. 2003). Using a BP, Swift et al. (1983) and Batchelder and Swift (1989) showed that zooplankton were usually major sources of epipelagic BL in the southern Sargasso Sea, except when the concentration of the BL dinoflagellate *Pyrocystis noctiluca* was high. In a study teaming a submersible and a High Intake Defined EXcitation (HIDEX) BP, Widder et al. (1999) were able to locate a thin layer composed of the copepod *Metridia* by its BL. The copepods were located near the thermocline where marine snow, a potential food source for the copepods, was temporarily trapped by the density discontinuity. Recently, a new generation of bathyphotometers was used to survey distinct plankton communities in Monterey Bay, a coastal region where both spatial and seasonal differences in the distribution of BL plankton occur (Haddock et al. 2004, 2002, 2001). These investigations show that BL integrated with other oceanographic measurements offer a further dimension to examine biological and ecological significance using the conventional suite of measurements.

With respect to the fine-scale organization of the BL coastal regime, the distribution of bioluminescence remains poorly understood due to limitations of the instruments used, which were typically designed for open-ocean applications. Bathyphotometers with high flow rates (18 L s^{-1} and higher), such as HIDEX (Widder et al. 1993; Neilson et al. 1995), were initially designed to ensure optimal capture efficiency in the open ocean where bioluminescent organisms vary widely in abundance and ability to avoid capture. In coastal waters, such high flow rates and large instruments might obscure the fine-scale distribution of bioluminescent organisms, and make it difficult to discriminate individual organisms amidst the bulk BL signal. Furthermore, the size of most large BPs requires large deployment vessels and dedicated winches, effectively barring them from use close inshore and on small mobile platforms or moorings. We suggest that smaller BPs with moderate flow rates are more appropriate for coastal research, where much of the BL is produced by dinoflagellates and populations of small zooplankters, particularly small copepods, larvaceans, cnidarians, and ctenophores.

In view of the unavailability of BPs to meet requirements for coastal research, we developed a BP to meet excitation and measurement requirements for this environment. The result is the small and relatively inexpensive Multipurpose Bioluminescence Bathyphotometer (MBBP) described here. It has undergone two generations of development, and through these instruments, we are advancing our understanding of the aggregate BL signal. As we show here, data collected from several MBBPs are repeatable with respect to spatial and temporal differences in the bioluminescent plankton class determined from the BP signal. The MBBP has a convenient small size, a power requirement easily supported by a battery pack when necessary, a high signal-to-noise ratio, and a strongly turbulent flow field for optimal stimulation. It has been successfully integrated on a greater variety of platforms than any previous BP including towed and shipboard profiling systems, stationary and profiling moorings, and on remotely operated vehicles and autonomous underwater vehicles (AUVs).

The MBBP was initially designed as a mid-body insert for an early prototype of the Remote Environmental Monitoring Units (Moline et al. 2005). It was first field tested in 1998 as a ship-based profiler in East Sound, Washington (Herren 2002; Herren et al. 2003, McManus et al. 2003) and in the Santa Barbara Channel. The MBBP has performed successfully on the MBARI remotely operated vehicles *Ventana* (Haddock et al. 2002), and on three classes of AUVs: the MBARI Odyssey-class AUV (Haddock et al. 2001), the Dorado-class AUV (Herren et al. 2003), and on later versions of the Woods Hole REMUS AUV, as an exchangeable nose cone module (Blackwell et al. 2002, Moline et al. 2005). MBBPs were deployed on two long-term moorings: the MBARI M1 mooring in Monterey Bay, CA (Haddock et al. 2001) and the Long-term Ecosystem Observatory (LEO) optical profiling node off the coast of New Jersey (Moline et al. 2000). A MBBP has been successfully integrated into the Ocean Response Coastal Analysis System, a profiling mooring (Donaghay et al. 2002) designed for thin-layer studies. For all deployment modes and configurations tested, intercalibration was maintained.

Materials and procedure

General MBBP specifications—The MBBP (Fig. 1) was designed as a small cylinder to minimize hydrodynamic disturbance when used as a stand-alone instrument and to facilitate incorporation into several compact instrument packages and platforms. The instrument is an assembly of seven sections milled from 15.24 cm diameter by 3.8 cm thick black polycarbonate discs. This allowed a compact design by avoiding space-consuming tubing connections between internal chambers. Section interconnections are sealed with O-rings and held together with stainless steel bolts. The MBBP was pressure tested in the field to a depth of 200 m, which is below the maximum nocturnal depth for the majority of coastal BL plankton (<100 m).

The MBBP measures BL in a light-baffled, approximately 500 mL detection chamber through which seawater is driven by an impeller delivering effective mechanical excitation to the entrained luminescent organisms (Fig. 1B). The in-house designed impeller pump (Fig. 1C) has a flooded rotor with a single axial gap. Low-relief impeller blades minimize fouling

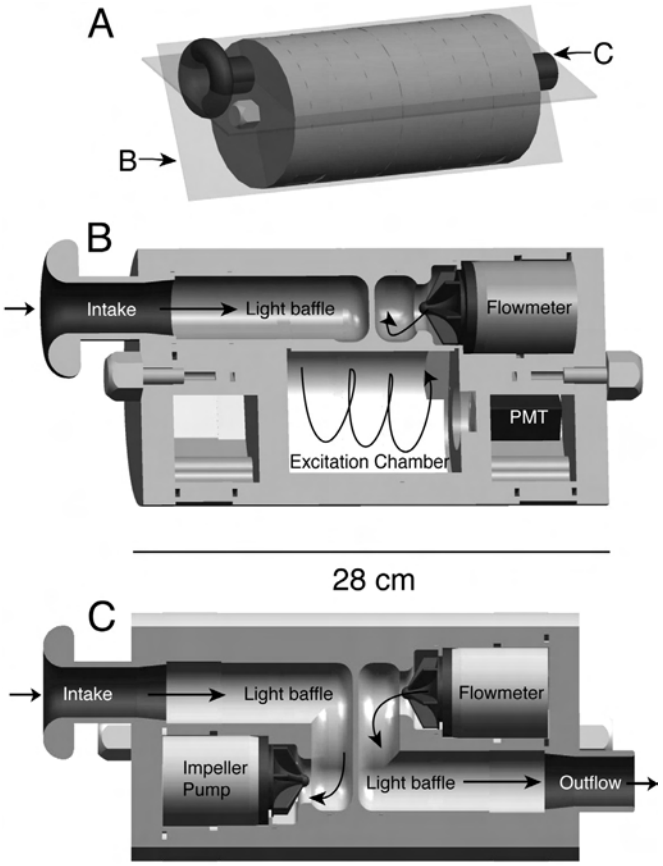

Fig. 1. MBBP three-dimensional diagram (A), with oblique gray planes intersecting the instrument to show orientation of cut-away views: (B) side view and (C) top view. Arrows and labels on views B and C show the flow path of water through the instrument. Water is drawn through the intake port, around a light-baffle, through the smooth blade impeller pump and down into the PMT detection chamber. The PMT is positioned to view the volume of the excitation chamber. Water is then pumped upwards from the chamber through the flow meter, around a second light baffle, and is expelled through the exhaust port.

by kelp and other filamentous algae common in coastal waters and provide ample shear force for mechanical excitation of plankton luminescence (Latz et al. 1994).

Residence time, the mean time a particle resides in the BP detection chamber, depends on chamber volume, pump efficiency, and flow rate (set by pump rotational rate). Pump revolutions per minute are regulated by measuring the period between power source phase changes and adjusting the pulse width modulation of the power to the windings of the in-house designed brushless DC pump motor. Following field tests, optimal pump speed was determined and set between 350 to 400 mL s^{-1}. Since the flow rate is affected slightly by the platform-dependent variation of water flow around the instrument, flow rate through the BP is continuously recorded by a custom Hall-effect flow meter. This allows for flow rate correction during data processing.

Light emitted by organisms within the chamber is detected with a Hamamatsu (H5783) photomultiplier tube (PMT), which has an integrated power supply and an 8-mm diameter window viewing the chamber. The spectral response is 300 to 650 nm, with peak sensitivity at 420 nm. System noise is almost all in the analog to digital converter and is on average less than one count out of 65536, full analog to digital converter scale. On the most sensitive range, one count typically represents less than 1×10^7 photons s^{-1} relative to an isotropic light source in the center of the chamber. Actual value, for each count, is determined during calibration and using this factor, data are corrected before incorporation into the serial output stream.

Light absorption by the interior detection chamber walls is minimized with either highly reflective gloss white Krylon paint (1501 Krylon Spray Enamels) or flat white Rust-Oleum paint (7590 Rust-Oleum Corp.), used only on the exchangeable AUV nose cone module. Reflectivity of coatings was measured using a Shimadzu UV-VIS 2401 spectrophotometer and integration sphere attachment (Spectralon coating, Labsphere, Inc.) with $BaSO_4$ as the reference, 100% reflectance. Krylon paint was 77% ± 4% reflective and Rust-Oleum was 78% ± 5% reflective. Both coatings were spectrally flat between 750 to 400 nm, covering the emission spectra of BL organisms. Krylon was found to damage the polycarbonate chamber wall while Rust-Oleum appeared to be more compatible with this material.

According to the deployment mode and platform, data may be transmitted to a deck computer in real time, stored internally in compact flash memory, or assimilated into host memory systems, as on profiling moorings or AUV platforms. The operational parameters of the system may be modified during deployment through an RS-232 serial connection, or set prior to deployment and stored in system memory. The MBBP can receive power from a deployment platform (0.5 amps) or from alkaline battery packs (12-18 V, with approximately 14 amp hours), contained in a separate data-logging vessel. The MBBP contains internal depth and temperature sensors, and supports external sensors such as fluorometers or optical backscattering sensors.

The performance of enclosed-volume, BL bathyphotometers is strongly affected by BL stimulation efficiency. This is the fraction of total mechanically stimulable light (TMSL) emitted by entrained organisms measured by the MBBP. This critical measurement is described below, along with demonstration of the following: visualization of flow internal to the instrument, PMT spatial responsively within the detection chamber, and BL potential as a function of flow rate. Finally, to illustrate the effectiveness of this instrument in defining the fine-scale organization of BL in coastal environments, examples of sea trials using the MBBP appear in the assessment section.

Stimulation efficiency—The outstanding characteristics of a bathyphotometer that affect BL stimulation efficiency are (1) the extent of signal loss by premature excitation in the BP intake, (2) the duration and intensity of excitation, and (3) residence

Table 2. Experiment conditions: dinoflagellate species, cell concentrations (cells mL^{-1}), syringe pump speed (mL s^{-1}), and sphere stimulation time (s)

Organism	Concentration (cells mL^{-1})	Injection speed (mL s^{-1})	Stirring speed (rpm*)	Sphere stimulation time (s)
P. fusiformis	25-26	0.83	510	60
L. polyedrum	645	0.13	1270	85

There were 10 replicates per experiment, and the volume in all replicate sample vials was 10 mL.
*Revolutions per minute.

time of organisms in the detection chamber. Critical light detector properties that affect this measurement are (1) sensing geometry, (2) radiant responsivity, and (3) measurement time constant. To compare BPs, it is important to determine the fraction of total mechanically stimulable light (TMSL) that a BP evokes from organisms under measurement.

In this study, stimulation efficiency was determined in the laboratory using cultures of two species of bioluminescent dinoflagellates, *Pyrocystis fusiformis*, and *Lingulodinium polyedrum* (formerly, *Gonyaulax polyedra*). The BL output of the dinoflagellates measured by the MBBP was compared to TMSL measurements made with a custom-built integrating sphere photometer system, referenced to a NIST-calibrated secondary light standard (Optronics Laboratories Inc.). A precision mechanical stimulator in the sphere permitted measurement of TMSL by running samples of test organisms to light extinction.

The duration of stimulation should be long enough to exhaust light output. This is a difficult measurement to optimize because in many organisms the pools of luminescent substrates may be exhaustible with differing time constants. Thus TMSL is affected by the species-specific response to both intensity and frequency of excitation (Bowlby and Case 1991; McDougall 2002; Widder et al. 1983). This poses an inevitable technical problem in all flow-through BP designs because they can only measure instantaneously excited luminescence. Some bioluminescence occurs before organisms reach the detection chamber, and nearly all bioluminescent organisms can produce additional light upon repeated stimulation. The theoretically ideal BP detection chamber would be large enough to retain all luminescent sources in view of the PMT until they have responded completely to the initial suprathreshold stimulus. The integrating-sphere system did measure TMSL emitted by the test organisms because they were stimulated to light exhaustion, 60 s for *P. fusiformis* and 85 s for *L. polyedrum* (Table 2). The difference between the two measurements (integrating sphere versus MBBP) takes into account the residence time of the excited cells in the MBBP and permits an estimation of the stimulation efficiency under the experimental conditions.

Cultured BL organisms—In the absence of conveniently culturable bioluminescent zooplankton, the two species of cultured bioluminescent dinoflagellates (*P. fusiformis* and *L. polyedrum*), with different response kinetics, were used to characterize stimulation efficiency of the MBBP. Dinoflagellate cultures were grown in F/2 media (Guillard and Ryther 1962) on a 12:12 light cycle, at 2000 μW cm^{-2} (92 μE m^2 s^{-1}), in a temperature-controlled incubator (18°C). The cell concentrations used for these experiments (Table 2) were chosen based on both PMT sensitivity limits and within reported ranges of cell concentrations in the ocean, from 50 to 25,000 cells mL^{-1} (Lewis and Hallett 1997) and below that of bloom conditions reported by Lapota (1998) and Sweeney (1975). The *P. fusiformis* culture originated in the Halmahera Sea, isolated by B. Sweeney in 1975, and has been maintained in our laboratory since that time. *L. polyedrum* was isolated from the Santa Barbara Channel, CA, USA, in 1995 (C. Stone, pers. comm. unref.).

Dinoflagellate samples from laboratory incubators were prepared 16 to 18 h before an experiment, during their minimally excitable photophase. A haemocytometer was used to determine the concentration of *L. polyedrum* (40 μm average diameter), and a Sedgewick-Rafter counting chamber was used to determine the concentration of *P. fusiformis* (1 mm average length) before and after the experiments. These two species are valuable for determinations of stimulation efficiency because they have distinctly different light-emission intensities and flash kinetics. The first flash of a quiescent *P. fusiformis* is approximately 5 times brighter than any immediate subsequent flashes and can last up to 210 ms. Subsequent flashes, which are dependent on excitation intensity and frequency, can last, in the aggregate, up to 650 ms (Widder and Case 1981). The BL emission of *P. fusiformis* is brighter (~10^{11} photons s^{-1} $cell^{-1}$) and lasts longer (50 s) than the flash pattern of *L. polyedrum* (~10^9 photons s^{-1} $cell^{-1}$ and 10 s flash duration) (Fig. 2). The dinoflagellate species used to test MBBP stimulation efficiency represent the variability in the BL signal encountered commonly in the coastal marine environment, where both rapid single flash kinetics (*L. polyedrum*) and longer, multi-flash kinetics (*P. fusiformis*) are observed.

Light-measuring instruments—To directly compare data from the MBBP and the integrating sphere photometer, a temperature-stabilized LED was placed in each instrument, and light output was measured at three light intensities. A linear relationship between the integrating sphere and MBBP response was calculated, using this intercomparison ($P < 0.001$, $R^2 = 0.99$).

Because there is a complex relation between stimulus strength, rate of stimulation applied, and TMSL in dinoflagellates (for detailed studies refer to McDougall 2002), the stimu-

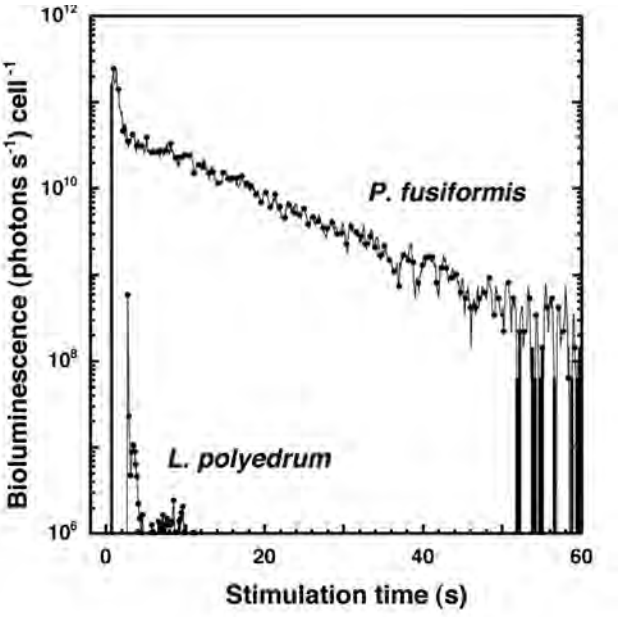

Fig. 2. Comparison of typical *P. fusiformis* and *L. polyedrum* flash kinetics (photons s^{-1} $cell^{-1}$) as measured by a custom-built integrating sphere photometer system.

lation intensity within each experiment was held constant and set below the level that causes damage to the cells. TMSL measured from samples stimulated in the integration sphere for each experiment are listed in Table 3. Light levels detected at the end of the stimulation period for all samples were indistinguishable from background counts recorded by the PMT (e.g., "exhaustion" light levels were within 2 standard deviations of averaged background counts (10^6 photons s^{-1} in the integrating sphere), per methods in Jenkins and De Vries 1970), indicating that mechanically excited BL capacity was exhausted for the specified excitation mode used during the stimulation period. TMSL measurements conducted in the integrating sphere photometer were recorded over a set time period determined for each species used (Table 2).

Experimental protocol—The protocol for stimulation efficiency measurements had two treatments and one control (Fig. 3). The control samples represented the cells' TMSL and consisted of quiescent cell samples stimulated in the integrating sphere only. Treatment one (T1) and treatment two (T2) samples were handled in the same manner prior to testing but were tested separately in the integrating sphere (T1) or the MBBP (T2). Comparison of control and treatment values gives (1) the fraction of dinoflagellate TMSL that was detected by the MBBP and (2) the fraction of TMSL that occurred prior to the experiment because of premature stimulation, not recorded by the MBBP.

There were two sources of premature stimulation in this experiment: (1) stimulation due to the sample delivery (handling) method and (2) stimulation due to the flow path from the intake port to the impeller, at the entrance to the MBBP detection chamber. Prestimulation due to the method of delivery was quantified by comparison of control and T1 samples. Flow path stimulation was quantified by comparison of T1 and T2 samples. In this way, the protocol allows differentiation between and quantification of each source of premature stimulation to determine the stimulation efficiency of the MBBP.

Prior to the experiment, control samples were prepared during cell photophase by dispensing 10 mL of the cell cultures into 15 mL glass scintillation vials. Samples for T1 and T2 were loaded into 60 mL syringes fitted to 30 cm length Tygon tubes (5 mm inner diameter, 60 mL volume). To ensure the same cell concentration and local environmental conditions among treatments and control, all samples were loaded and dispensed at the same flow rate (0.83 mL s^{-1}) using a syringe pump (Model 351, Sage Instruments).

Post-experiment cell counts showed that this loading method did not cause significant differences in cell concentrations between or within each treatment. Because BL was stimulated as the cells flowed past the narrow syringe mouth, even at the lowest flow rates of the syringe pump, only the volume of cells in the Tygon delivery tubes was used for the treatment samples. The cells were not observed to flash, even with image intensification, as they traveled through the remainder of the tube into the sample vial or into the MBBP intake port. At an injection rate of 0.83 mL s^{-1} (Table 2), the wall shear stress inside the tubes during delivery was calculated to be 0.09 dyne cm^{-2}, well below the 1 dyne cm^{-2} threshold for stimulating dinoflagellate bioluminescence (Latz et al. 1994).

After samples were prepared, they were stored in an incubator until the experiment, at 18°C for *L. polyedrum* and 21°C for *P. fusiformis* (environmental temperature ranges found in Steidinger and Tangen 1997; Polat and Sarihan 2000). Samples were transferred with minimum mechanical agitation to the

Table 3. Biological calibration of MBBP: comparison of control, T1, and T2 TMSL values, used to calculate stimulation efficiency of the MBBP [(T2/T1) × 100] and stimulation inefficiency of delivery method 100 – [(T1/Control) × 100] using both *P. fusiformis* and *L. polyedrum**

	Control TMSL (photons × 10^{10})	T1 TMSL (photons × 10^{10})	T2 TMSL (photons × 10^{10})	Stimulation efficiency of MBBP (%), T1 vs T2	Inefficiency of delivery method (%), T1 vs control
P. fusiformis	950 ± 23	740 ± 1.6	262 ± 4.1	35	22
L. polyedrum	42.1 ± 19	5.97 ± 1.0	1.03 ± 0.8	17	83

*Stimulation efficiency is the ratio of TMSL measured by the integrating sphere (T1) to BL potential measured by the MBBP (T2). Inefficiency of delivery method is the percent of control TMSL that was excluded from T1 TMSL values, due to prestimulation during sample delivery method.

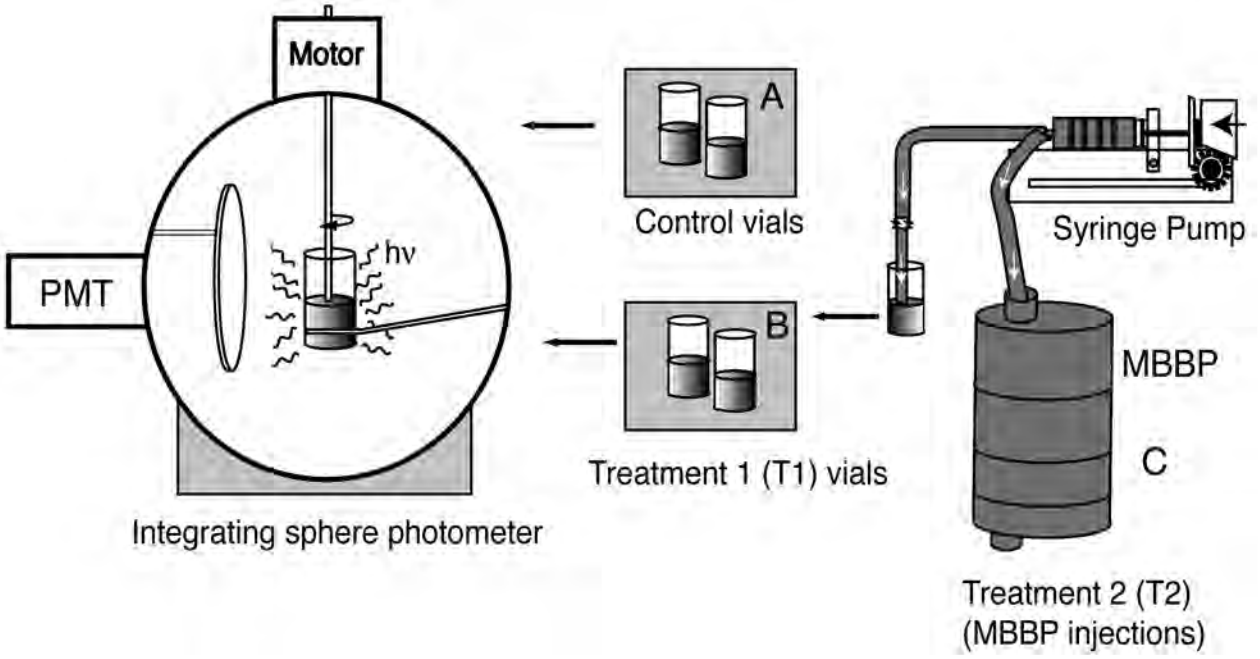

Fig. 3. Diagram of the delivery and measurement protocol for the stimulation efficiency experiment. (A) An undisturbed 10 mL control volume is tested for TMSL in the integrating sphere. (B) Treatment 1 (T1): a 10-mL volume is dispensed from a syringe-tube into a vial and TMSL was measured. (C) Treatment 2 (T2): a 10-mL volume, from the same syringe-tube as T1, was dispensed into the MBBP intake port for measurement of BL potential.

adjacent experiment room and allowed 45 min to recover from inadvertent stimulation. For this experiment, TMSL of control samples was determined in the integrating sphere system (Fig. 3A). T1 and T2 samples were delivered to the integrating sphere or MBBP respectively using the syringe pump (Fig. 3B and 3C). For a more detailed description of this procedure, see Herren 2002 (pp 14-16 and 43-47).

Flow visualization and residence time—A portion of the flow path in the MBBP was observed with image intensification to determine the location of maximum BL excitation along the flow path and to qualitatively characterize the type of flow inside the chamber (Fig. 4). A clear polycarbonate faceplate replaced the normal opaque endplate so that the impeller and the entire cylindrical detection chamber were visible. In a darkroom with the entire instrument submerged in a seawater tank and with the pump running, the syringe pump injected *P. fusiformis* into the intake port of the instrument. An intensified silicon intensifier target (ISIT) camera (MTI VE 1000, DAGE, Inc.) recorded the paths of cells as traced by their BL emissions. When low cell concentrations were used (<20 cells mL^{-1}), individual cell paths could be tracked in the video for the duration of their flashing episodes using motion analysis software (MetaMorph, Universal Imaging Corporation).

We then examined the temporal match of the MBBP bioluminescence signal with the ISIT-video recorded flow path of the dinoflagellates through the instrument. Flow paths of luminescing *P. fusiformis* in the detection chamber were videotaped, as described previously, while concurrent measurements of the BL signal were made using the MBBP detection electronics (Fig. 4). An empirical calculation of the residence time of discrete glowing particles in the MBBP was made from injection of discrete aliquots of the dinoflagellates into the flow path of the instrument while simultaneously recording the BL signal and ISIT video.

PMT spatial responsivity—The responsivity of the PMT to point-source illumination throughout the MBBP detection chamber was experimentally measured. The fraction of the MBBP detection chamber volume viewed by the PMT was measured with a small, isotropic, blue LED light source positioned at 24 uniformly distributed positions in the detection chamber, and the PMT responses were recorded.

Assessment

Stimulation efficiency—BL stimulation efficiency calculations for the dinoflagellate test organisms show that the MBBP captured a greater percentage of the TMSL from *P. fusiformis* (35%) than from *L. polyedrum* (17%) (Table 3). Stimulation efficiency is determined by the ratio of TMSL measured by the MBBP (T2) to that measured by the integrating sphere (T1). The fraction of light measured by the MBBP is commonly referred to as BL potential. The effects of prestimulation solely caused by the instrument design were removed from the stimulation efficiency calculations by subtracting the values of T2 from T1. From these results, we conclude that the MBBP recorded more of the light emitted by the brighter, multiple-flash dinoflagellates and perhaps undersampled or understimulated the BL of

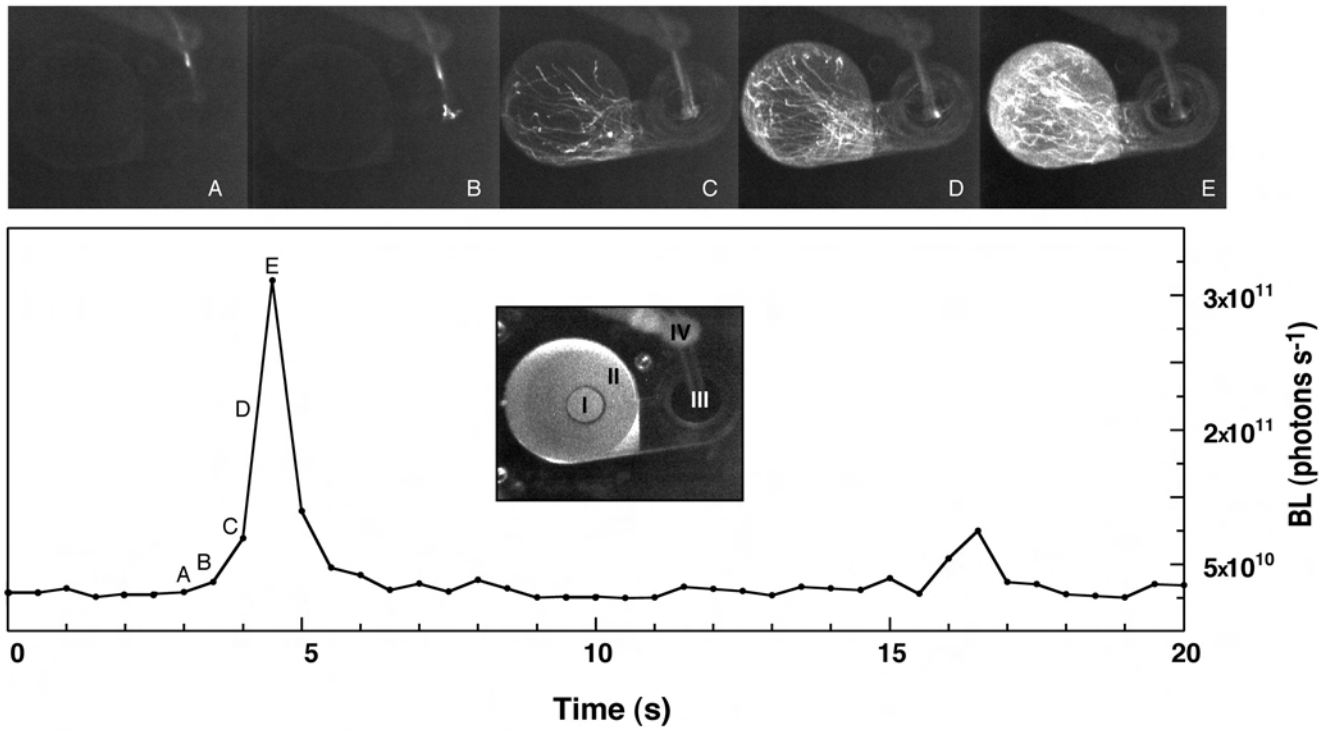

Fig. 4. Visual tracking of BL cell paths of dinoflagellates flowing through the MBBP excitation chamber (A-E), matched temporally with a graph of the measured BL potential (photons s^{-1}). Inset in the graph is the MBBP field of view, shown under full light (I-IV). (I) PMT face in detection chamber, (II) detection chamber, (III) entrance to impeller pump with smooth blades, (IV) clear tube that delivered dinoflagellates volume to the MBBP. The black border is the outer diameter of the instrument exterior. (A) Dinoflagellates are stimulated at the curve of the injection tube. The first cells arrive at the impeller (B), before entering the chamber (C). Cell numbers increase in the chamber (D) as the main volume of cells travel through the instrument. Maximum BL potential occurs (E). Note that the BL emission in the pump region is very small compared to that occurring inside the chamber.

dinoflagellates that emit fewer and lower intensity flashes. The inefficiency of the delivery method, defined as the percent of TMSL lost from T1 due to prestimulation relative to that of the control TMSL, was lower on average for *P. fusiformis* (22%) than for *L. polyedrum* (83%) (Table 3).

Flow visualization and residency time—Video analysis of bioluminescent dinoflagellates in the flow path of the MBBP shows very little BL was emitted at the impeller, prior to cells entering the detection chamber. This is consistent with the excitation latency of these cells (Widder and Case 1981). Figure 4 shows the time course of a defined volume of cells (approximately 200 cells mL^{-1}) traveling through the instrument. The video frame image, inset in the graph, is viewed under bright light and illustrates the field-of-view for the other frames in Fig. 4A to 4E, which are illuminated only by bioluminescence. In this image, the Roman numerals show the location of (I) the PMT window, (II) the white cylindrical wall of the detection chamber, (III) the impeller, and (IV) the cell delivery tube and holder. A small fraction of cells was excited at the bend in the delivery tube (A), continued to glow on reaching the impeller (B), and were projected into the detection chamber (C-D). The location of maximal BL emission inside the detection chamber was both a consequence of the location of maximal excitation at the impeller and of the response latency of the cells (Fig. 4E).

The temporal correlation of luminescent cells traveling along the flow path and their resulting BL as measured by the MBBP was examined. Flow paths of flashing *P. fusiformis* in the detection chamber were videotaped while concurrent measurements of BL potential were made using the MBBP (Fig. 4, graph). BL signal peaks are congruent in time with video frames (Fig. 4, A-E). These results show the MBBP is well-suited for sampling situations requiring fast detection times, for example, as in detection of thin layers of coastal bioluminescent plankton (McManus et al. 2003).

Flow through the chamber was qualitatively characterized as turbulent from the complex cell paths in the video data. Luminescent cell paths appear to be randomly distributed as cells are transported throughout the chamber. Motion analysis revealed that the BL emission tracked per cell lasted an average of 7.5 ± 3.0 frames or approximately 225 ms (n = 172). Since the average duration of a dinoflagellate flash is 260 ± 10 ms, these results suggest that the first flash of *P. fusiformis* occurred completely inside the detection chamber. In addition, secondary flashes along cell tracks were observed in 5% of the video frames, and probably were recorded by the PMT

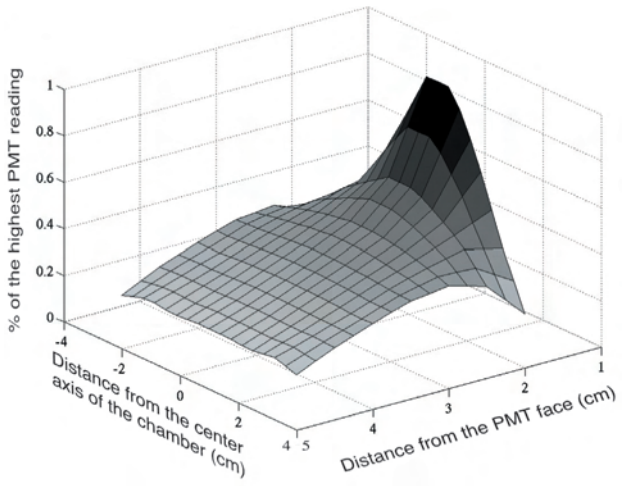

Fig. 5. Surface plot of PMT readings (photons s^{-1}) as a function of blue-wavelength LED location (n = 24) across the width (0.89-cm increments) and length (1.2-cm increments) of the excitation chamber. Values are represented as a percent of the highest value recorded by the PMT.

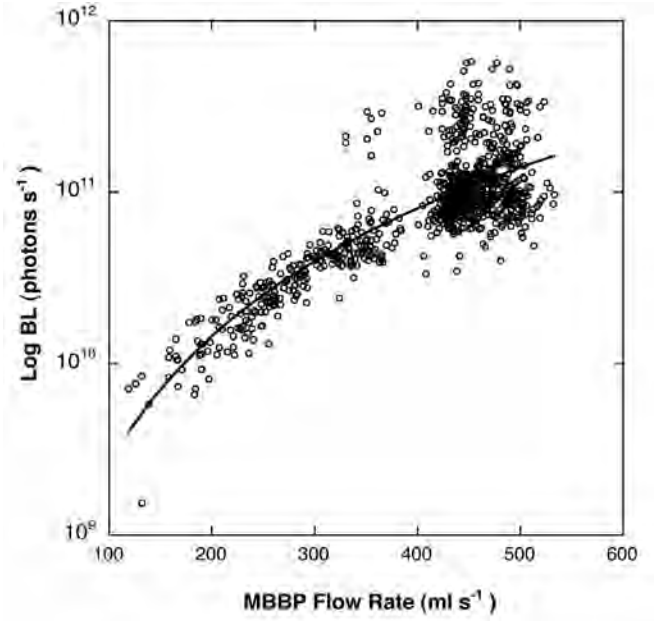

Fig. 6. BL signal as a function of MBBP pumping rate (P) as measured in the field. The MBBP was held at a fixed depth for 10 min while pumping rates were increased. A power curve was fit to the data (BL = 31813 $*P^{2.4959}$, R^2 = 0.65).

as well. These secondary flashes are thought to result from the high level of turbulence existing throughout the detection chamber, causing further excitation.

The residence time of the MBBP, defined as the time a particle resides in the detection chamber, was both empirically and theoretically determined. Fig. 4 illustrates the decay of the BL signal over time after a discrete volume of *P. fusiformis* cells was injected into the detection chamber. The empirically derived residence time (10.4 ± 4.5 s, n = 24) for the MBBP was longer than the theoretically calculated residence time (6.6 s), which was calculated as follows.

If we assume a well-mixed chamber with volume V (L), with an initial concentration of particles, m_0 (approximate number of particles), and then introduce a flow of particle-free water at a flow rate of q (mL s^{-1}), the concentration of particles (m_t) in the chamber will decrease according to the relationship (e.g., Boyce and Di Prima 2002):

$$m_t = e^{\left(\frac{-qt}{V}\right)} m_0$$

where m_t is the concentration of particles remaining in the chamber at time t (residence time variable). Solving for t we obtain:

$$t = -\frac{V \ln\left(\frac{m_t}{m_0}\right)}{q}$$

If an initial concentration of 100 particles (m_0 = 100) is instantaneously input into the MBBP chamber volume (V = 0.5 L) at a known flow rate (q = 0.35 L s^{-1}), 1% of the population (1 particle) would remain after flushing the MBBP with particle-free water for 6.6 s, which is the theoretical residence time. Given an initial concentration of 1000 particles, one particle would remain in the chamber after 9.9 s.

PMT spatial responsivity—Results from PMT spatial response tests show that as the location of the LED changed, along both the length and width axes of the detection chamber, the PMT response changed (Fig. 5). The highest responsivity was observed at the core of the cylindrical chamber and at the PMT faceplate. Responsivity diminished as the LED was moved toward the edges of the chamber and away from the PMT faceplate. In the next iteration of design, the PMT will have a light baffle placed so that any light reaching the PMT will be repeatedly reflected, thus reducing positional bias and improving the use of flash intensity as a discriminator of major groups of luminescent organisms.

Field experiments—In BP design, there is an obvious trade-off between pumping a large enough sample volume to statistically determine plankton concentrations, and collecting high-resolution spatial data that correctly represents the fine-scale structure of bioluminescence present in the water column (Case et al. 1993). In order to find optimal pumping rates, TMSL was measured in relation to flow rate and profiling speeds. The MBBP instrument was held at a fixed depth for 10 min while flow rate was increased from 125 to 525 mL s^{-1} (Fig. 6). The data were fit to a power curve (BL = 31813 $*P^{2.4959}$, R^2 = 0.65).

The variability of data points markedly increased at pumping rates greater than 400 mL s^{-1} (Fig. 6). This may indicate that larger mesozooplankton were entrained at the maximum flow rates tested. However, in addition to increased variability at these higher flow rates, the slope of the power curve decreased as well. Thus, increased flow rates did not result in proportionally increased levels of BL past a certain rate (400 mL s^{-1}). We

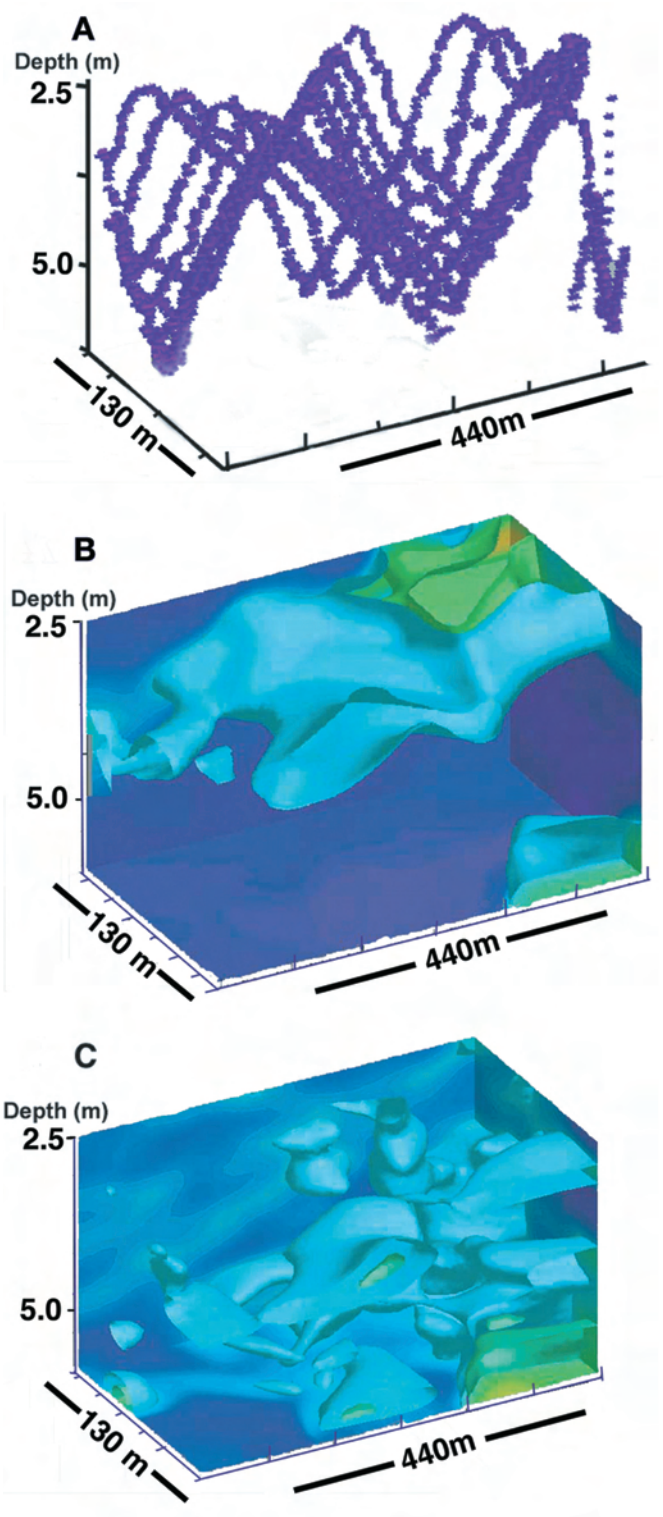

Fig. 7. Comparison of BL and fluorescence structure concurrently collected on a REMUS AUV off the New Jersey coast in July 1999 by an MBBP and an independent fluorometer. Color contour plots are interpolations of data collected as the AUV traveled through a box-shaped volume of water in an undulating pattern (A). Isosurfaces of high FL (B) and BL (C) show that the two signals occur in spatially distinct patches.

propose this occurred because organisms were expelled from the detection chamber more quickly than at lower flow rates. Even though more organisms were sampled per unit time, a smaller fraction of each organism's TMSL was measured at flow rates greater than 400 mL s^{-1}. Thus, the empirically determined flow rate (400 mL s^{-1} ± 20 mL s^{-1}) was kept constant on the following studies. Based on results of optimal flow rate and residence time, the descent rate for profiling-platform MBBPs was set to 10 cm s^{-1} (~5 data points per 0.5 m). This vertical profiling rate allowed accurate measurement of small-scale features such as thin layers (e.g., McManus et al. 2003) and highly stratified frontal regions.

LEO-15 HYCODE field study—A MBBP was integrated into a REMUS AUV (Moline et al 2005) along with fluorescence (FL, Seapoint), conductivity, temperature and depth (CTD, Ocean Sensors), and optical backscatter (OBS, Seapoint) sensors. This MBBP was the first BP to be integrated into an AUV, and the resulting BL measurements represent the highest spatial resolution BL data collected by that time. Initial tests were conducted at the Long-term Ecosystem Observatory at 15 m (LEO-15) near the Rutgers University Marine Field Station in July 1999 during the Hyperspectral Coupled Ocean Dynamics Experiment (HyCODE). The AUV was programmed to traverse a volume of water (~90 m by 222 m by 5 m depth) in an undulating sampling pattern and collected BL and FL data (Fig. 7). Three-dimensional tracks of the AUV mission (Fig. 7A) are shown with color interpolations of fluorescence (B) and BL data (C).

At the LEO-15 site, BL was not strictly colocated with the FL signal, indicating multiple distinct BL communities distributed over a very small volume (Fig. 7). While there were areas of overlap between the two signals, the majority of the chlorophyll-containing organisms were found in a layer in the upper 2 m of the imaged volume (Fig. 7B). In contrast, the BL signal had a more patchy distribution mainly located in the lower 2 m of the volume (Fig. 7C). Since the distribution of BL and FL were not identical in this case study, each instrument revealed a different subset of the plankton community.

MUSE field study—During the MUSE experiment conducted in Monterey Bay, CA, in September 2000, three MBBPs collected BL data from several platforms including the MBARI Odyssey-class AUV (developed by J. Bellingham, MBARI) and two shipboard profiling packages. The AUV instrumentation included a fluorometer, CTD, OBS, and MBBP. High-resolution data were concurrently collected by the AUV as it traveled from onshore to offshore of Santa Cruz, CA (Figs. 8, 9). With the MBBP positioned inside the flooded hull of the AUV, water was pumped in and out through flush-mounted external ports on opposite sides of the hull, approximately 1 m behind the nose, as dictated by the AUV instrumentation load.

The vertical structure of the fluorescence (Fig. 8A) and BL data (Fig. 8B-D) measured by AUV-mounted, independently plumbed optical sensors was coherent along the 5-km survey, especially at their upper depth limits. However, the high values of BL continued below the lower boundary of the chlorophyll

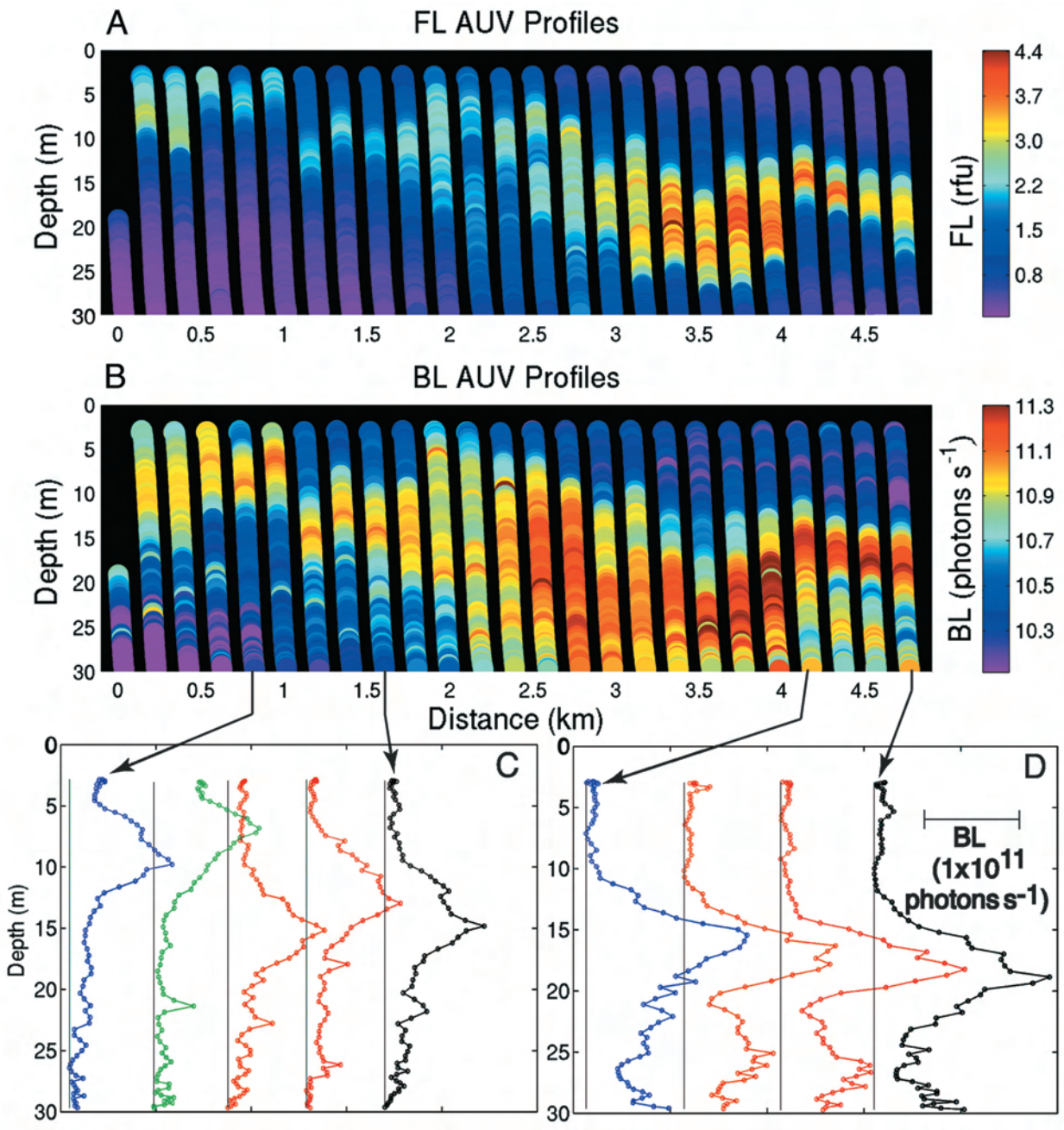

Fig. 8. Coherence of fluorescence data (A) and BL data from an MBBP collected by an AUV in Monterey Bay, CA, in September 2000. The vertical structure (A, B) measured by these independently plumbed optical sensors matched well across the 5 km survey, especially at their upper depth limits. The same BL features were repeatedly detected in a subset of adjacent downcast profiles (C, D), as demonstrated by their similar shapes over depth.

maximum. This pattern in vertical structure was commonly found throughout our studies from 2000 to 2004. The consistency of measurements made by the MBBP was demonstrated by its ability to repeatedly detect distinct BL features (peaks and valleys) in profiles separated by more than 0.5 km (Fig. 8C, D). Although the absolute depths of these features varied as a function of the water column physical environment (e.g., thermocline depth), the shape of the profiles was retained.

The stacked, color contour plots (Fig. 9A, B) show two 1.8 km segments (map in Fig. 9E) of interpolated temperature, BL, and FL data. Although the CTD and fluorometer were fed by a separate water intake from the MBBP, they detected the same sharp physical transition detected by the BP (Fig. 9A). In the nearshore segment (Fig. 9A, C) bioluminescence was closely correlated with FL, with a Gaussian-like distribution centered around the depth of the thermocline. These were most likely

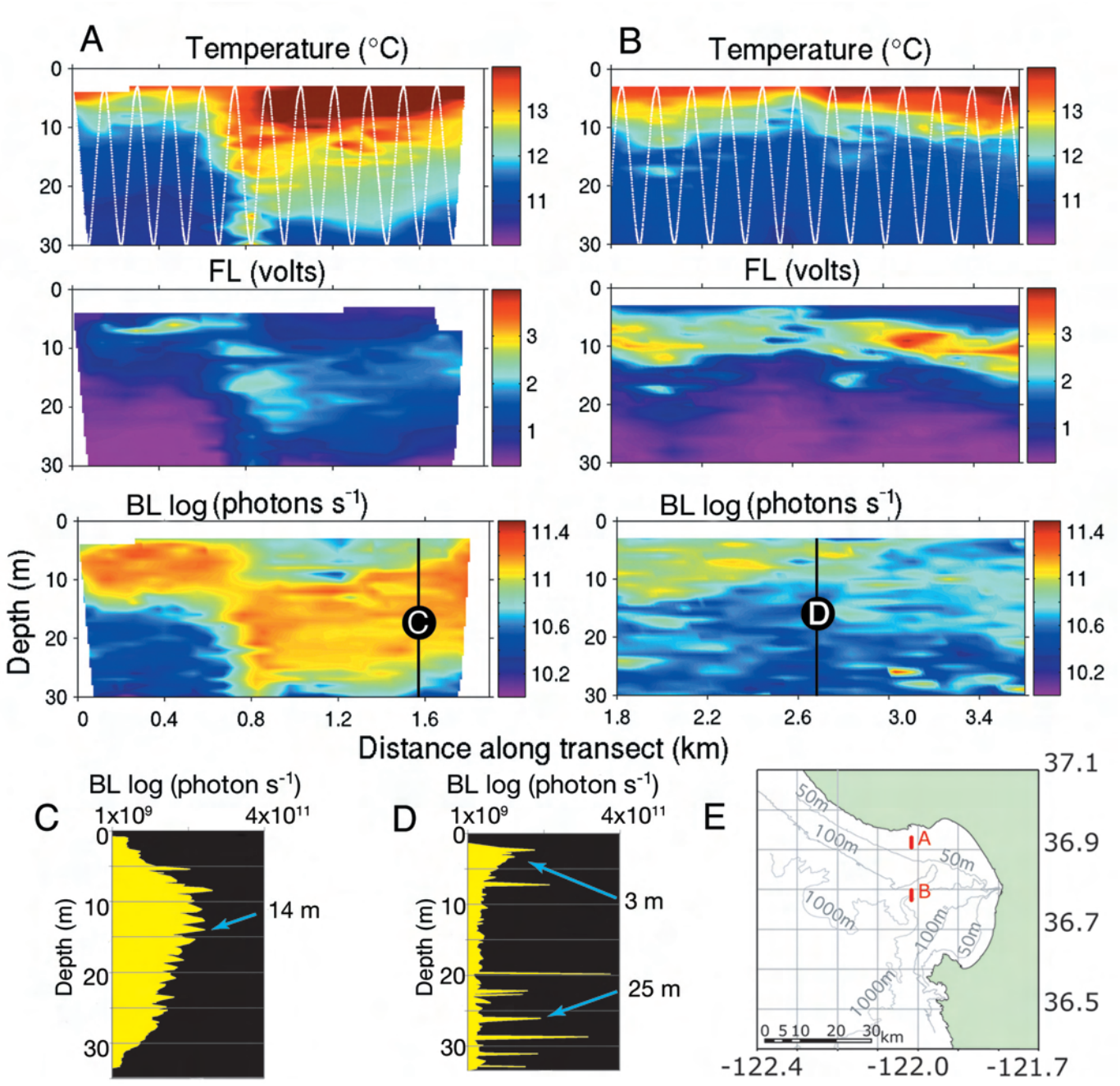

Fig. 9. Comparison of temperature, fluorescence, and BL collected by an AUV in Monterey Bay, CA, in September 2000. The AUV path is overlaid on the temperature plots (white line), and on the map (E). The degree of correlation between BL and FL can change from strong (A) to weak (B) within a single survey. Shipboard profiles of BL over depth (m) (C and D) and discrete plankton samples (blue arrows) were collected independently, at the locations denoted by black-circled C and D.

caused by high concentrations of bioluminescent dinoflagellates that emitted relatively low-intensity flashes. As the AUV traveled further offshore, the distribution of BL became decoupled from FL, and the signal consisted of fewer but brighter flashes, indicative of less abundant zooplankton sources with greater BL capacity (Fig. 9B, D). This interpretation is further supported by discrete-depth plankton samples (blue arrows in Fig. 9C, D) collected by a Schindler-trap (Schindler 1969; Pagano and Saint-Jean 1989) deployed independently of the AUV. Between these two sections, the ratio of BL copepods to non-BL copepods increased from onshore to offshore (13.5% to 20%), and further offshore increased to 30% (not shown).

Discussion

Bioluminescence measurements by BPs represent a fraction of the TMSL from entrained organisms. This fraction depends on biological excitation characteristics and on the stimulation efficiency, the type of mechanical excitation, and the residence time of the BP. The overall efficiency of any BP must be known if its signal is to bear any determinable relationship to the total possible luminescence in the sampled body of water. For this reason, the MBBP and HIDEX BP series have been carefully evaluated in terms of their excitation efficiency as described here and by Widder et al. (1993). The only comparable evaluation of a BP listed in Table 1 was performed by Swift et al. (1985). MBBP and HIDEX evaluations have been limited to two culturable dinoflagellate species (*P. fusiformis* and *L. polyedrum*), which have different excitation responses. As opportunity occurs, the MBBP series can be tested against collected specimens of luminescent zooplankton. Ultimately, this effort might allow calculation of an accurate BL light budget for specific locales. This approach, however, will be complicated by the complex BL signals produced by many zooplankters. For example, the large midwater copepod *Gaussia princeps* can emit multiple fast flashes and a luminous cloud when given a single stimulus (Bowlby and Case 1991).

A drawback to the use of small BPs is that most have short residence times relative to large volume BPs (Widder et al. 1993). With its intermediate-size detection chamber volume and flow rate, the MBBP design optimizes excitation through initial impeller shear and subsequent turbulence in the chamber. In combination, these features allow some fraction of the sample volume a greater residence time, as compared to HIDEX, derived to be approximately 10 s from experiments described above. Finally the design of the inlet flow path, the contour of which is a trade-off between reduction of ambient light reaching the detection chamber and prevention of premature excitation is a critical element of BP design. The curvature of the MBBP intake path was optimized to reduce the effects of both constraints, and functions in daylight near the surface without ambient light contamination.

Bioluminescence, evoked by excitation, is a complex signal compared to other oceanographic signals that allow direct measurement, such as temperature, salinity, solar-derived light signals, and concentrations of chlorophyll-containing organisms responsible for bulk FL signals. Therefore, BP design represents a compromise between measurement resolution and broad spatial coverage. Bathyphotometers with high flow rates and large detection chambers will capture larger quantities of rare, evasive, and fast-swimming species, but faster profiles and higher flow can obliterate fine structure in the water column. In comparison, data from specialized small instruments such as the MBBP usefully reveal plankton distributions within the water column, allowing researchers to differentiate between key classes of organisms responsible for the large majority of BL in coastal waters.

It was not possible to determine the excitation efficiencies of bioluminescent copepods, larvaceans, ctenophores, radiolarians, larval euphausiids, or small cnidarians experimentally. All are organisms sampled by the MBBP, and each species would probably be unique in the fraction of its TMSL registered by the BP. Such measurements under laboratory conditions are difficult to make without culturable species. Isolation and testing of specimens from field collections, made in the past for ecosystem light budget estimates, is extremely laborious because of the time required to isolate individual specimens from water samples aboard a ship. Additional time and resources are needed for the organisms to recover undisturbed in a dark incubator before shipboard measurement of TMSL (Batchelder and Swift et al. 1989).

As demonstrated by the MUSE and LEO sea trial data, the MBBP was able to sample BL structure in coastal zones on a scale not previously possible (cm to m and over many km). The versatility of the MBBP was demonstrated by deployment on advanced platforms, such as AUVs, where it could detect the presence of both luminescent zooplankton (characterized by larger flashes) and luminescent phytoplankton or microzooplankton (characterized by smaller flashes). In the future, we anticipate higher order analysis of the MBBP signal, such as flash-kinetic processing or signal "decoding," may permit adaptive changes in sampling strategy, reduced need for sample collection for taxonomic identification, and thus more efficient use of ship time.

Comments and recommendations

Measurement of fine-scale BL features such as those documented here would not be possible without an instrument such as the MBBP, a device that only minimally disturbs water column structure while accurately registering fine-scale BL features. Rigorous laboratory calibration and extensive field-testing have shown the MBBP to be a versatile and reliable instrument, useful in many deployment modes. Of the entire list of BPs from Table 1, it and the HIDEX series BPs are the most extensively tested in the laboratory and at sea. It is well suited for studies in coastal ocean zones, and it may be well employed for studies in the euphotic zone of the open-ocean where bioluminescent organisms are usually found in greater concentrations. In summary, the MBBP is presented as an instrument of value in studying the fine-scale spatial distribution of some bioluminescent organisms, currently a critical matter under investigation by plankton ecologists, biological oceanographers, and ecosystem modelers. Its adaptability to many deployment modes invites general use by oceanographers as an addition to their instrumentation suite. Our intention is to optimize this instrument class and seek to make it available for general oceanographic use, leading perhaps to a greater understanding of why bioluminescence is so prevalent in the sea.

References

Aiken, J., and J. Kelly. 1984. A solid state sensor for mapping and profiling stimulated bioluminescence in the marine environment. Cont. Shelf Res. 3(4):455-464.

Batchelder, H. P., and E. Swift. 1989. Estimated near-surface mesoplanktonic bioluminescence in the western North Atlantic during July 1986. Limnol. Oceanogr. 34(1):113-128.

———, ———, and K. J. R. Van. 1990. Pattern of planktonic bioluminescence in the northern Sargasso Sea: Seasonal and vertical distribution. Mar. Biol. 104(1):153-164.

———, ———, and ———. 1992. Diel patterns of planktonic bioluminescence in the northern Sargasso Sea. Mar. Biol. 113(2):329-339.

Blackwell, S. M., and others. 2002. A new AUV platform for studying near shore bioluminescence structure, p. 197-200. *In* P. E. Stanley and L. J. Kricka [eds.], Twelfth international symposium on bioluminescence and chemiluminescence. World Scientific Publishing Co.

Bivens, J. R., M. L Geiger, and J. L. Bird. 2002. Interpreting bathyphotometer signals, p. 1705-1710. *In* Proceedings from Oceans 2002 IEEE/MTS, 29–31 October 2002, Biloxi, Mississippi, USA.

Boden, B. P., E. M. Kampa, and J. M. Snodgrass. 1965. Measurements of spontaneous bioluminescence in the sea. Nature. 208:1078-1080.

Bowlby, M. R., and J. F. Case. 1991. Flash kinetics and spatial patterns of bioluminescence in the copepod *Gaussia princeps*. Mar. Biol. 110(3):329-336.

Boyce, W. E., and R. C. DiPrima. 2002. Elementary differential equations and boundary value problems. Wiley. 768 pp.

Buskey, E. J. 1992. Epipelagic planktonic bioluminescence in the marginal ice zone of the Greenland Sea. Mar. Biol. 113:689-698.

Case J. F., S. H. D. Haddock, and R. D. Harper. 1995. The ecology of bioluminescence, p. 115-122. *In* A. K. Campbell, L. J. Kricka, and P. E. Stanley [eds.], Bioluminescence and chemiluminescence: fundamentals and applied aspects. Wiley.

——— and others. 1993. Assessment of marine bioluminescence. Nav. Res. Rev. XIV 2:31-41.

Clark, G. L., and M. G. Kelley. 1965. Measurements of diurnal changes in bioluminescence from the sea surface to 2,000 meters using a new photometric device. Limnol. Oceanogr. 10:R54-R66.

Donaghay, P. L., J. M. Sullivan, C. Moore, B. Rhoades, and M. A. McManus. 2002. Four-dimensional measurement of the fine-scale structure of inherent optical properties in the coastal ocean using the ocean response coastal analysis system (ORCAS). Ocean Optics XVI, 18–22 November 2002, Santa Fe, New Mexico, USA.

Fucile, P. D. 1996. A low cost bioluminescence bathyphotometer. Gulf of Maine Ecosystem Dynamics Symposium, September 11-16, St Andrew's, New Brunswick, USA.

Geistdoerfer, P., and A. -M. Vincendeau. 1999. A new bathyphotometer for bioluminescence measurements in the Armorican continental shelf (Northeastern Atlantic). Oceanologica Acta. 22:137-151.

Gitel'zon, J. I., L. A. Levin, A. P. Shevirnogov, and R. N. Utyushev. 2000. Bioluminescent patrolling of marine ecosystems—Bioalarm, p. 59-62. *In* J. F. Case, P. J. Herring, B. H. Robison, S. H. D. Haddock, L. J. Kricka, and P. E. Stanley [eds.], Eleventh International Symposium on Bioluminescence and Chemiluminescence. World Scientific Publishing Co.

Greene, C. H., E. A. Widder, M. J. Youngbluth, A. Tamese, and G. E. Johnson. 1992. The migration behavior, fine structure, and bioluminescent activity of krill sound-scattering layers. Limnol. Oceanogr. 37(3):650-658.

Greenblatt, P. R., D. F. Feng, A. Zirino, and J. R. Losee. 1984. Observations of planktonic bioluminescence in the euphotic zone of the California current. Mar. Biol. 84:75-82.

Guillard, R. R. L., and J. H. Ryther. 1962. Studies of marine planktonic diatoms. I. Cyclotella nana Hustedt and Detonula confervacea Cleve. Can. J. Microbiol. 8:229-239.

Haddock, S. H. D., M. A. Moline, C. M. Herren, E. L. Heine, J. G. Bellingham, and J. F Case. 2001. AUV-measured distribution of bioluminescence in a coastal environment. American Society of Limnology and Oceanography, Albuquerque, NM, USA, February 12-16.

———, E. A. Widder, M. A. Moline, J. G. Bellingham, and J. F. Case. 2002. High-resolution measurements of coastal bioluminescence using autonomous and remotely operated vehicles. Ocean Sciences, Honolulu, HI, USA, February 11-15.

———, C. M. Herren, J. Brewster, C. Orrico, and J. F Case. 2004. Distribution of bioluminescence and zooplankton in Monterey Bay, CA. American Society of Limnology and Oceanography, Honolulu, HI, USA, February 13-19.

Hall, A. F., and R. F. Staples. 1978. Bathyphotometer measurements of vertical bioluminescence in the NE Atlantic during May 1977. U.S. Naval Oceanographic Office, Technical Note: 3005-3-78, 27 pp.

Hastings, J. W. 1983. Biological diversity, chemical mechanisms, and the evolutionary origins of bioluminescent systems. J. Mol. Evol. 19:309-321.

Herren, C. M. 2002. Bioluminescent plankton: association with thin layers and marine snow in coastal oceans, Ph.D. thesis. University of California, Santa Barbara.

———, A. L. Alldredge, and J. F. Case, 2003. Coastal bioluminescent marine snow: fine structure of bioluminescence distribution. Cont. Shelf Res. 24:413-442.

Herring, P. J. 2002. The biology of the deep ocean. Oxford University Press.

Jenkins, R. H., and B. De Vries. 1970. Worked examples in X-ray spectrometry. Springer-Verlag.

Lapota, D., C. Galt, J. R. Losee, H. D. Huddell, J. K. Orzech, and K. H. Nealson. 1988. Observations and measurements of

planktonic bioluminescence in and around a milky sea. J. Exp. Mar. Biol. Ecol. 119(1):55-82.

———, M. L. Geiger, A. V. Stiffey, D. E. Rosenberger, and D. K. Young. 1989. Correlation of planktonic bioluminescence with other oceanographic parameters from a Norwegian fjord. Mar. Ecol. Prog. Ser. 55(2-3):217-228.

———, D. K. Young, S. A. Bernstein, M. L. Geiger, H. D. Huddell, and J. F. Case. 1992. Diel bioluminescence in heterotrophic and photosynthetic marine dinoflagellates in an Arctic Fjord. J. Mar. Biol. Assoc. U. K. 72(4):733-744.

———. 1998. Long-term and seasonal changes in dinoflagellate bioluminescence in the Southern California Bight. Ph.D. thesis. University of California, Santa Barbara.

Latz, M. I., J. F. Case, and R. L. Gran. 1994. Excitation of bioluminescence by laminar fluid shear associated with simple couette flow. Limnol. Oceanogr. 39(6):1424-1439.

Lewis, J., and R. Hallett. 1997. Lingulodinium polyedrum (*Ganyaulas polyedra*), a blooming dinoflagellate. Oceanog. Mar. Biol. 35:97-161.

Lieberman, S. H., D. Lapota, J. R. Losee, and A. Zirino. 1987. Planktonic bioluminescence in the surface waters of the Gulf of California [Mexico]. Biol. Oceanogr. 4(1):25-46.

Losee, J. D., D. Lapota, and S. H. Lieberman. 1985. Bioluminescence: A new tool for oceanography. p. 211-234. *In* A. Zirino [ed.], Mapping strategies in chemical oceanography. Advances in chemistry series 209. American Chemical Society.

Losee, J., K. Richter, S. Lieberman, and D. Lapota. 1989. Bioluminescence: Spatial statistics in the North Atlantic. Deep-Sea Res., Part A. 36(5):783-802.

Marra, J., and E. O. Hartwig. 1984. Biowatt: A study of bioluminescence and optical variability in the sea, Eos Trans. AGU 65:732-733.

McDougall, C. A. 2002. Bioluminescence and the actin cytoskeleton in the dinoflagellate *Pyrocystis fusiformis*: an examination of organelle transport and mechanotransduction. Ph.D. thesis. University of California, Santa Barbara.

McDuffey, A., and J. L. Bird. 2002. The underway survey system at the Naval Oceanographic Office. *In* Proceedings from Oceans 2002 IEEE/MTS, 29–31 October 2002, Biloxi, Mississippi, USA. p. 1705-1710.

McManus, M. M., and others. 2003. Changes in characteristics, distribution and persistence of thin layers over a 48-hour period. Mar. Ecol. Prog. Ser. 261:1-19.

Moline, M. A., E. Heine, J. F. Case, C. M. Herren, and O. Schofield. 2000. Spatial and temporal variability of bioluminescence potential in coastal regions, p.123-126. *In* J. F. Case, P. J. Herring, B. H. Robison, S. H. D. Haddock, L. J. Kricka, and P. E. Stanley [eds.], Eleventh International Symposium on Bioluminescence and Chemiluminescence, World Scientific Publishing Co.

——— and others. 2005 (in press). Remote environmental monitoring units: An autonomous vehicle for characterizing coastal environments. J. Atmos. Ocean. Tech.

Nealson, D. J. 1985. Bio-optical measurement platforms and sensors. STD-R-1160. Johns Hopkins University, Applied Physics Laboratory.

Neilson, D. J., M. I. Latz, and J. F. Case. 1995. Temporal variability in the vertical structure of bioluminescence in the North Atlantic Ocean. J. Geophys. Res. C: Oceans Atmos. 100(C4):6591-6603.

Rudyakov, Y. A. 1968. Bioluminescent potential and its relationship to luminous plankton concentration. Oceanology 8(5):710-714.

Pagano, M., and L. Saint-Jean. 1989. Comparison of two methods for sampling zooplankton, the net and the Schindler trap, in Ebrie Lagoon (Ivory Coast). Hydrobiologia 173(3): 167-172.

Piontkovski S. A., Y. N. Tokarev, E. P. Bitukov, R. Williams, and D. A. Kiefer. 1997. The bioluminescent field of the Atlantic Ocean. Mar. Ecol. Prog. Ser. 156:33-41.

Polat, S., and E. Sarihan. 2000. Seasonal changes in the phytoplankton of the Northeastern Mediterranean (Bay of Iskenderun). Turk. J. Biol. 24:1-12.

Schindler, D. W. 1969. Two useful devices for vertical plankton and water sampling. J. Fish. Res. Board Can. 26(7):1948-1955.

Seliger, H. H, W. G. Fastie, and W. D. McElroy. 1969. Towable bathyphotometer for rapid area mapping of concentrations of bioluminescent marine dinoflagellates. Limnol. Oceanogr. 14:806-813.

Shulman, I., S. H. D. Haddock, D. J. McGillicuddy, Jr., J. D. Paduan, and P. W. Bissett. 2003. Numerical modeling of bioluminescence distributions in the coastal ocean. J. Atmos. Ocean. Tech. 20:1060-1068.

Soli, G. 1966. Bioluminescent cycle of photosynthetic dinoflagellates. Limnol. Oceanogr. 11(3):355-363.

Steidinger K. A., and K. Tangen. 1997. Dinoflagellates, p. 509-510. *In* C. R. Thomas [ed.], Identifying marine phytoplankton. Academic Press.

Sweeney, B. M. 1975. Red tides I have known, p. 225-234. *In* V. R. LoCicero [ed.], First international conference on toxic dinoflagellate blooms. The Massachusetts Science and Technology Foundation.

Swift, E., W. H. Biggley, P. G. Verity, and D. T. Brown. 1983. Zooplankton are major sources of epipelagic bioluminescence in the Southern Sargasso Sea. Bull. Mar. Sci. 33(4):855-863.

———, E. J. Lessard, and W. H. Biggley. 1985. Organisms associated with stimulated epipelagic bioluminescence in the Sargasso Sea and the Gulf Stream. J. Plankton Res. 7:831-848.

———, J. Van Keuren, H. P. Batchelder, C. R. Booth, and C. P. Li. 1988. A moored instrument to measure stimulated and natural oceanic bioluminescence. Int. Soc. Optical Eng. (SPIE) 925:76-86.

———, J. M. Sullivan, H. P. Batchelder, J. Vankeuren, R. D. Vaillancourt, and R. R. Bidigare. 1995. Bioluminescent organisms and bioluminescence measurements in the North

Atlantic Ocean near latitude 59.5°N, longitude 21°W. J. Geophys. Res., C: Oceans Atmos. 100(C4):6527-6547.

Tarasov, N. I., and J. I. Gitel'zon. 1961. Comprehensive investigation of luminescence in the sea during scientific expeditions [Russian]. Byul. Okeanogr. Kom. (ANSSSR). 8:75-80.

Utyushev, R. N., L. A. Levin, and J. I. Gitel'zon. 1999. Diurnal rhythm of the bioluminescent field in the ocean epipelagic zone. Mar. Biol. 134(3):439-448.

Widder, E. A., and J. F. Case. 1981. Two flash forms in the bioluminescent dinoflagellate, *Pyrocystis fusiformis*. J. Comp. Physiol. A. 143:43-52.

———, M. I. Latz, and J. F. Case. 1983. Marine bioluminescence spectra measured with an optical multichannel detection system. Biol. Bull. Mar. Biol. Lab. 165(3):791-810.

———, C. H. Greene, and M. J. Youngbluth. 1992. Bioluminescence of sound-scattering layers in the Gulf of Maine. J. Plankton Res. 14(11):1607-1624.

———, J. F. Case, S. A. Bernstein, S. MacIntyre, M. R. Lowenstine, M. R. Bowlby, and D. P. Cook. 1993. A new large volume bioluminescence bathyphotometer with defined turbulence excitation. Deep-Sea Res. Part I 40(3):607-627.

———, S. Johnsen, S. A. Bernstein, J. F. Case, and D. J. Neilson. 1999. Thin layers of bioluminescent copepods found at density discontinuities in the water column. Mar. Biol. 134:429-437.

Submitted 21 July 2004
Revised 13 January 2005
Accepted 30 March 2005